TELKOMNIKA, Vol.17, No.4, August 2019, pp.2107~2115
ISSN: 1693-6930, accredited First Grade by Kemenristekdikti, Decree No: 21/E/KPT/2018
DOI: 10.12928/TELKOMNIKA.v17i4.12939

Enhanced symmetrical split ring resonator for metallic surface crack detection

Rammah A. Alahnomi*[1], Z. Zakaria*[2], Zulkalnain Mohd Yussof[3], Tole Sutikno[4], Ammar Alhegazi[5], Ahmed Ismail Abu-Khadrah[6]
[1,2,3,5]Center for Telecommunication Research and Innovation (CeTRI), Universiti Teknikal Malaysia Melaka (UTeM), Hang Tuah Jaya, Durian Tunggal, Melaka, Malaysia
[4]Department of Electrical Engineering, Universitas Ahmad Dahlan, Yogyakarta, Indonesia
[6]College of Computing & Informatics, Saudi Electronic University, Saudi Arabia
*Corresponding author, e-mail: alrammah89@gmail.com[1], zahriladha@utem.edu.my[2]

Abstract

An enhanced sensor based on symmetrical split ring resonator (SSRR) functioning at microwave frequencies has been proposed in order to detect and characterize the metal crack of the materials. This sensor is based on perturbation theory, in which the dielectric properties of the material affect the quality factor and resonance frequency of the microwave resonator. Conventionally, coaxial cavity, waveguide, dielectric resonator techniques have been used for characterizing materials. However, these techniques are often large, and expensive to build, which restricts their use in many important applications. Thus, the enhanced bio-sensing technique presents advantages such as high measurement sensitivity with the capability of suppressing undesired harmonic spurious and permits potentially metal crack material detection. Hence, using a High Frequency Structure Simulator (HFSS) software, the enhanced sensor is modeled and the reflection S11 is performed for testing the aluminum metal with crack and without crack at the frequency range of 100 MHz to 3GHz. Variation of crack width and depth has been investigated and the most obvious finding emerged from this study is that the ability of detecting a minimum of sub-millimeter crack width and depth which is a round 10 μm width or depth where the minimum shift of reflected frequency is recorded at 6.2 MHz and 3 MHz for crack width and depth respectively. The enhanced SSRR provides high capability of detecting small crack defection by utilizing the interaction between coupled gap resonators and it is useful for various applications such as aircraft fuselages, nuclear power plant steam generator tubing, and steel bridges and for others that can be compromised by metal fatigue.

Keywords*: crack, detection, microwave sensor, symmetrical split ring resonator (SSRR)*

Copyright © 2019 Universitas Ahmad Dahlan. All rights reserved.

1. Introduction

Recently, researchers have shown an increased interest in microwave sensors since they are desirable for many important applications such as food industry applications, quality control, surface crack detection, bio-sensing applications and solid and liquid materials detection [1–11]. Microwave planar based sensors can meet the demand in these devices technologies. This is due to their advantages including high field penetration and sensitivity in characterizing the properties of small electric materials. Microwave planar sensors are easy to fabricate, design, and cost effective. The planar sensor mechanism is based on measuring shifts in resonance frequencies and reflection coefficients when interacting with tested material samples. Defects in metallic materials such as steel bridges, gas and oil tubing and nuclear power plant steam generator turbines can be affected by cracks. Inspection and detection for surface and subsurface cracks in metallic materials is critical for the maintenance and assessment of the quality as supported by study in [12]. Numerous studies have attempted to use microwave sensors for crack detections [12-18].

In [16], authors investigated the crack detection in the surface of the metallic using waveguide sensor. An artificial intelligence was implemented to detect the crack from non-cracked surfaces in metallic materials. The waveguide sensor has the ability to observe any frequency changes or shifts in the magnitude of the reflection coefficient (S11) pattern. Those sensors achieve high accuracy rate however, they have a complex design and expensive to build. Another study done by [13], authors presented an electromagnetic bandgap

Received December 9, 2018; Revised April 18, 2019; Accepted May 10, 2019

inspired scanning-probe sensor for characterizing high frequency dielectric laminates. The material under test (MUT) is placed between the substrate comprising of 50Ω microstrip line and the electromagnetic bandgap which consists of 1x3-unit cell elements. Research finding by [15] also points towards crack detection which is consistent with literature [12]. Both research findings are using planar microwave sensor techniques based on complementary split ring resonator (CSRR). The CSRR is etched out from the ground of substrate and is excited by a microstrip line. A defected aluminum plate with crack can be scanned by passing it over the CSRR sensor where the near field will be distrusted, and the resonant frequency will be shift downwards.

The SSRR with/without spurline filters based sensors is initially reported in [1, 19, 20] and it is used for detecting the properties of solid materials such as FR4, Roger 5880 and Roger 4350. The sensor is successfully tested and have capability of detecting materials properties. Further investigation of possible enhancement and improvement of Symmetrical split ring resonator is indicated in [20]. The result demonstrates significant improvement in resonant frequency and reflection coefficients when the coupling gap between the feedlines and rings of the sensor is enhanced. Several types of schemes for material measurement techniques development have been analyzed and the enhanced coupling periphery technique has the highest performance since its insertion loss is low compare to others and has less shifted frequency as indicated in [20]. Thus, the integration of enhanced coupling periphery scheme and SSRR sensor is used for crack detection in this paper since it has much more performance and produces a maximum field perturbation with high sensitivity due to the coupling gap between the feedlines and ring structure. The enhanced SSRR sensor is used to detect small defected crack in metal materials. An investigation of sensor performance is carried out by varying out the depth and width of crack in the tested metal. The previous model of crack has been used to detect 100 μm cracks and in this work cracks smaller than this is being investigated.

2. Research Method

2.1. Enhanced SSRR Sensor Design

Figure 1 shows a schematic view of a square SRR formed with metallic strips of width, wf, and the radius of the inner and outer rings are denoted as R_i and R_o, respectively, measured from the centre of the structure. The splits on the inner and outer rings have identical gap dimensions g, respectively, lying diametrically on opposite sides of the same axis. A comparison of the simulated result between the split ring resonator (SRR) and enhanced symmetrical split ring resonator (SSRR) is demonstrated in Figure 2 where there is about 20 MHz shifting in reflected frequency. However, it can be clearly seen that the enhanced symmetrical split ring resonator has much more better sensitivity compared to split ring resonator (more details for slits and split can be found in [21]).

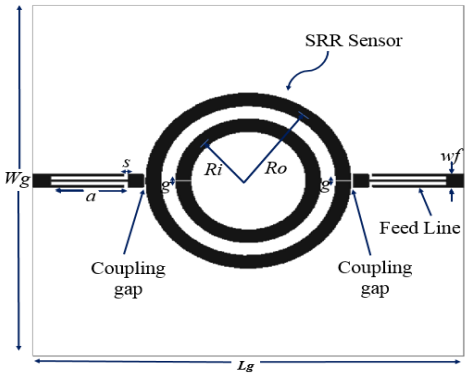

Figure 1. Schematic view of a circle split ring resonator (SRR) formed with metallic rings of width, wf and split gap dimensions, *g*

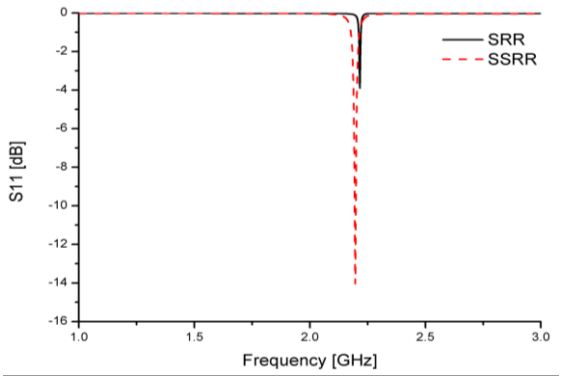

Figure 2. A comparison results of simulated minimum reflection for both split ring resonator (SRR) and enhanced symmetrical split ring resonator (SSRR)

The configuration and design parameters of SSRR structure are demonstrated in Figure 3 based on the mathematical equations from (1) to (3). It illustrates the relative positions of the feed lines and rings on the upper surface of the board. The feed lines and rings resonator are printed transmission lines with width chosen for 50Ω characteristic impedance [22]. A small gap g is included between the ring and each feed line; this gap is included to separate the resonant behavior of the ring from the feed network and ranges from 0.1 to 1.0 times the width of the feed microstrip. Roger corporation® RT/Duroid 5880 was used with substrate thickness of 0.787 *mm* (*h*), loss tangent of 0.0009 (tanδ), and permittivity of 2.20 (ε_r), refer to. It has a copper thickness of 17.5 *μm* (*t*). A cross-sectional dimension of 68.3 *mm* x 71.84 *mm*, (*Wg, Lg*) respectively, is used to model the proposed sensor with 0.37 *mm* (*g*) gap between the ring and feed-lines. The design structure of SSRR has a main ring radius of 15.85 *mm* of the outer ring and 10.85 *mm* main radius of the inner ring. The proposed sensor is modelled in the High Frequency Structural Simulator (HFSS) at 2.2 GHz operating frequency, and the simulation is carried out to obtain the two-ports scattering parameters in the specified frequency band.

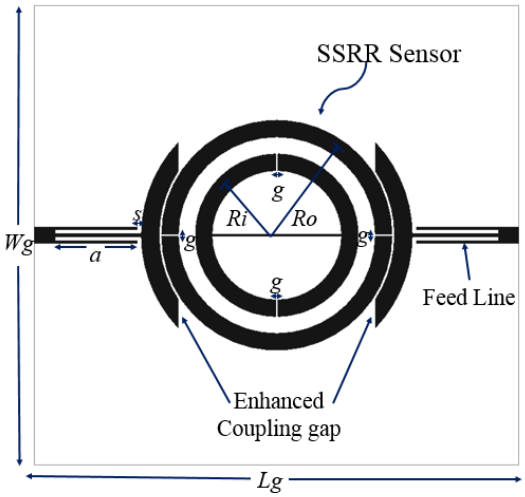

Figure 3. Design Structure of Enhanced Coupling gap SSRR sensor with 50 Ω loaded feedlines and the substrate is Roger RT/Duriod 5880 with thickness *h* = 0.787 *mm* and dielectric constant ε_r = 2.2. Dimensions are *Lg* = 71.84 *mm*, *Wg* = 68.3 *mm*, *R* = 15.85 *mm*, *a* = 12.76 *mm*, and for the gap *g* = 0.37 *mm*

The resonance in the conventional microstrip planar ring resonator is produced whenever the ring mean circumference is equal to an integral multiple of the guided wavelength:

$$2\pi r = n\lambda_g \tag{1}$$

where *n = 1, 2, 3, 4*… and so on. The resonant frequency for n modes can be calculated by using:

$$\lambda_g = \frac{\lambda}{\sqrt{\varepsilon_{eff}}} \tag{2}$$

where:

$$\lambda = \frac{c}{f}$$

So, by considering (1) and (2), the resonant frequency can be found using:

$$f_0 = \frac{nc}{2\pi r\sqrt{\varepsilon_{eff}}} \quad (3)$$

where r: the main radius of the ring element
λg: the guided wave length
n: the mode number, 1,2,3, ...
f_o: the resonant frequency
ε_{eff}: the effective of dielectric constant
c: the speed of the light (3×10^8)

For the 50 Ω characteristic impedance Zo, analysis of the ring structure begins with (ε_{eff}) is found by applying a formula found in [22, 23] for the appropriate value of the ratio of w to d:

$$\frac{w}{d} = \frac{8e^A}{e^{2A} - 2} \quad (4)$$

where:

$$A = \frac{Z_o}{60}\sqrt{\frac{\varepsilon_r + 1}{2}} + \frac{\varepsilon_r - 1}{\varepsilon_r + 1}\left(0.23 + \frac{0.11}{\varepsilon_r}\right)$$

$$\varepsilon_{eff} = \frac{\varepsilon_r + 1}{2} + \frac{\varepsilon_r - 1}{2}\frac{1}{\sqrt{1 + 12\left(\frac{d}{w}\right)}}$$

For the main radius, it can be calculated using this formula:

$$r = \frac{n\lambda_g}{2\pi} \quad (5)$$

It can be considered to be simple *LC* circuit with a response frequency fo using the following [24, 25]:

$$f_o = \frac{1}{2\pi\sqrt{L_r\left(C_r + C_g\right)}} \quad (6)$$

where, f_o is the SSRR resonant frequency, *Lr* and *Cr* are the inductance and capacitance associated with SSRR, respectively, *Cg* is the capacitance between the ground plane and microstrip-line. The *Cg* and *Lr* are always considered as constant due to the MUT which is usually non-magnetic, and a constant permittivity used in the substrate of the proposed sensor.

The effects of band-stop spurlines filters are applied to the symmetrical split ring resonator (SSRR) for harmonic suppression. This feature makes the proposed SSRR ring resonator compact and more suitable for microwave devices compared to other techniques. The configuration is embedded by L-shape slot with a length (*a*) and with a gap width (*s*). The frequency response is determined by optimizing the parameters: length (*a*), and gap (*s*). Generally, the slot width (*s*) or the gap exhibits the effects of the capacitive while the microstrip line provides an effect of the inductance. The length (*a*) dictates the frequency of the notch characteristic. The rejected wavelength can be calculated as [26]:

$$a = \frac{\lambda_g}{4} \tag{7}$$

where a = the spurline length, and λg = the rejected wavelength. By deriving (7) into the frequency domain as follows [26]:

$$f_{stop} = \frac{c}{4a\sqrt{\varepsilon_{eff}}} \tag{8}$$

where a = the spurline length, ε_{eff} = the effective permittivity of the substrate, c = speed of light ($3x10^8$ *m/s*), and f_{stop} = the undesired frequency.

2.2. Realization of Sensing Element

For obtaining a maximum electric field, enhanced coupling gap is applied to symmetrical split ring resonator with double spurlines. The coupling scheme is applied for enhancing the E-field distributions surrounding the SSRR sensor and achieving a maximum electric field. The coupling gap between the SSRR ring and feed lines are take into consideration due to its capacitive effects on changing the resonance frequency significantly. The SSRR with double spurlines sensor was fed through an enhanced coupling gap between the ring and the length of the microstrip feedlines.

Investigating the behavior of the field surrounding the enhanced SSRR resonator by showing the electric field distributions is significant for demonstrating the critical location at which the maximum E-field is concentrated. Figure 4 demonstrates the maximum electric field distribution on enhanced SSRR which can be used as a sensing element in order to place the material under test (MUT). The MUT will disturb the perturbing electric field which causes a shift in the resonance frequency. The shift is dependent on the material disturbing the electric field and it happens due to the real part and imaginary part of the material permittivity.

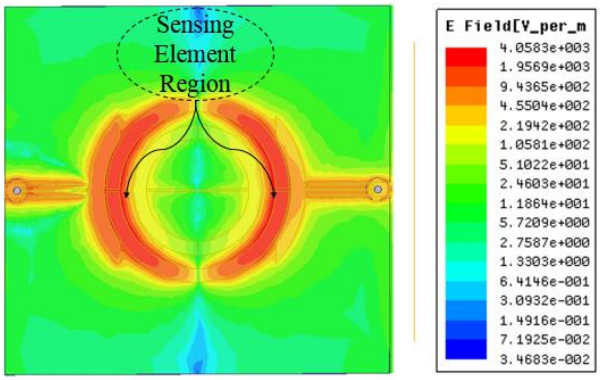

Figure 4. Simulated electric field distribution on an enhanced SSRR and the location of sensing element

2.3. Scanning Mechanism

A geometrical structure of the designed sensor and tested aluminum metallic plate with and without crack is described in Figure 5. For loaded condition, an overlay thin Teflon film with a thickness of 0.076 *mm* and 2.1 dielectric constant is used to conceal the surface of an aluminum plate which possibly hide the crack from visual inspections. The reason behind using Teflon film as a cover for the aluminum plate surface is that the tested material might be covered by a layer of dielectric coating or paint as discussed in [12].

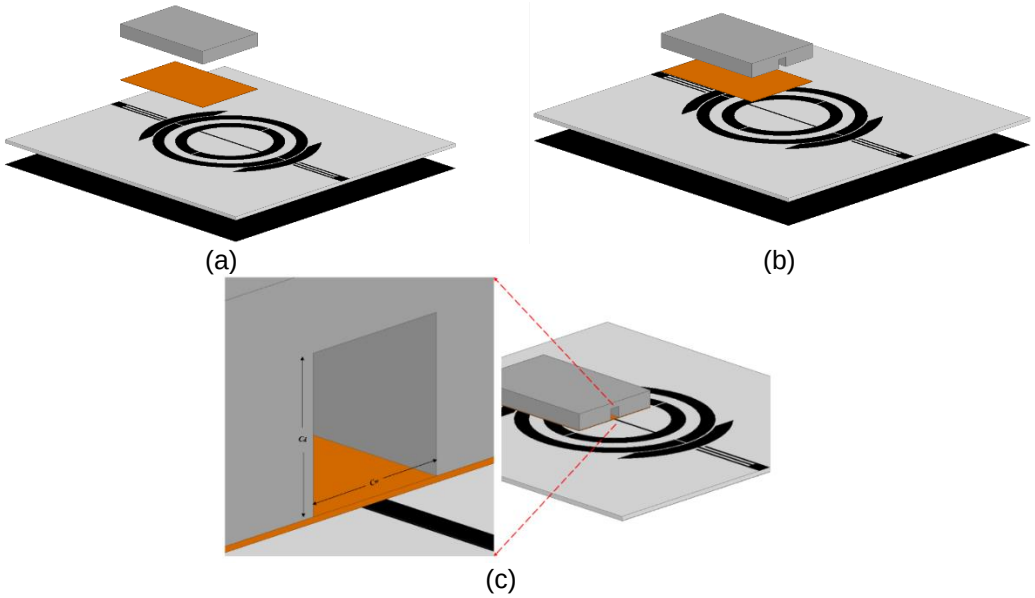

Figure 5. Design structure of enhanced SSRR sensor along with tested aluminum metallic plate: (a) Without crack, (b) with crack, (c) Crack depth and width

The sensing mechanism is performed by passing the sensor above the cracked aluminum metallic plate. Figure 6 demonstrates the scanning direction of the sensor in the aluminum metallic with crack. The distribution of electric field on the aluminum metallic plate with crack is also demonstrated in Figure 6. It demonstrates very high concentrated electric field on the surface of the cracked aluminum plate.

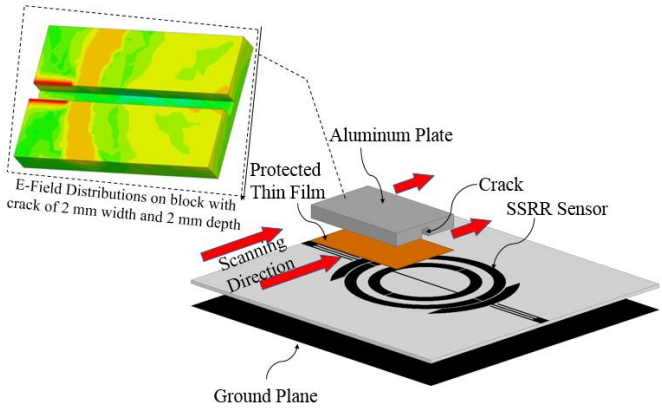

Figure 6. Scanning direction and the concentrated electric field on the surface of the cracked aluminum plate

3. Results and Discussions

The proposed enhanced SSRR is designed and simulated using High Frequency Structure Simulator (HFSS). The simulated results demonstrate the differences between the frequency response when the sensor is passed over the aluminum metallic with variation of crack width and depth. The sensor is scanned over the aluminum plate and the reflection coefficients are recorded when there is no crack under the senor and when the sensor passes over the cracks.

The effect of using another protected material on reflection coefficients (*S11, dB*) are studied in order to compare with a Teflon thin film as indicated in Figure 7. The protected coating materials is having a specification with a dielectric permittivity of 2.2 and 2.7, and a thickness of 0.13 *mm*, and 0.076 *mm* for the thin Teflon and Fast film; respectively. The obtained simulation result of the two protected materials is verified by a good agreement with the theoretical results which indicates that increasing the value of material permittivity, the shift in resonance frequency will be increased. The simulated results of using thin Teflon film is having a higher sensitivity with low resonant frequency shift compared with using Fast-film material since it has a higher value of permittivity. Thus, thin Teflon Film is suitable to be applied as a protected coating material for the enhanced sensor.

The result of reflection response with/without sample is demonstrated in Figure 8. It can be clearly seen that there is a shifting when the protected thin Teflon film is applied which is about 12 MHz. Furthermore, when the sensor scanning the aluminum metallic plate with no crack the reflected frequency is shifted up to 1 GHz from the operating frequency at 2.1965 GHz. However, a shift of more than 96 MHz from the reference case (aluminum with no crack) is achieved when there is a crack with 2 *mm* width and 2 *mm* depth on the aluminum metallic plate.

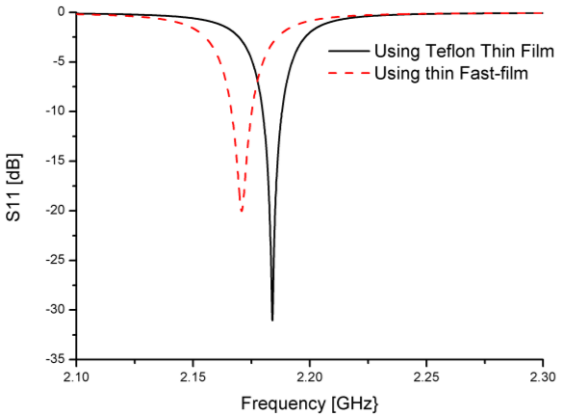

Figure 7. the frequency of minimum reflection when the sensor passes over a protected thin Teflon film and thin Fast film

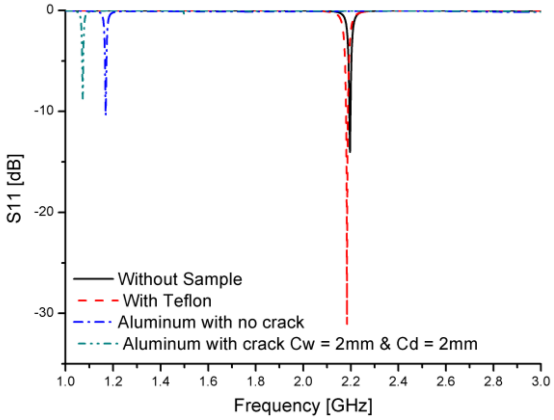

Figure 8. The frequency of minimum reflection when the sensor passes over a protected thin Teflon film, aluminum with no crack, and aluminum with crack width *Cw* =2 *mm* and depth *Cd* = 2 *mm*

A variation of the width and depth of the crack is considered and investigated in order to demonstrate the potential of this approach and its suitability for the application. The crack width was varied from 10 *μm* to 20 *μm* while keeping the crack depth fixed at 1 *mm*. Figure 9 demonstrates the effect of the reflected frequency by varying the width of crack and keeping the depth of crack constant. There is a clear trend of shifted resonant frequency at 10 μm and 20 um crack width. These shifts in the material properties are very important in detection purposes. The evidence from this study provides that the frequency response shift is about 6.2 MHz and 8 MHz when changing the crack width to 10 *μm* and 20 *μm*, respectively while keeping the depth to 1 *mm*. This indicates that this sensor can detect a 10 *μm* minimum of sub-millimeter crack width.

On the other hand, the width is keep constant at 1 *mm* while varying the value of crack depth to 10 *μm* and 20 *μm*. Figure 10 illustrates the ability of the proposed sensor to discriminate between two closely spaced cracks of depth at 10 *μm* and 20 *μm*. This is clearly demonstrated that the proposed sensor has the capability to resolve sub-millimeter cracks. The result of this study indicates that the frequency response shifts about 3 MHz and 11.7 MHz at 10 *μm* and 20 *μm* crack depth respectively, while keeping the width constant at 1 *mm*.

The purpose of this investigation is to determine the minimum crack depth that this sensor can detect which is make capable to be applied in very important industrial application.

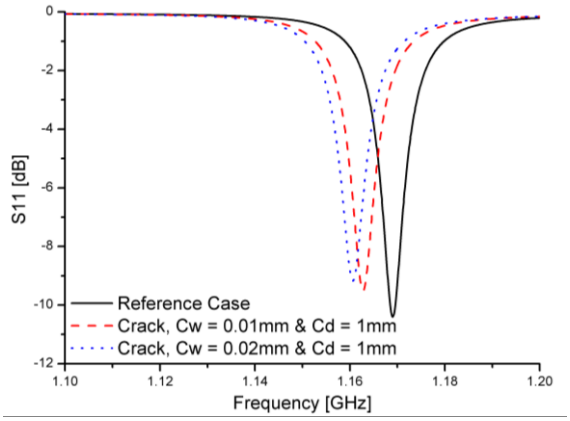

Figure 9. Variation of crack width *Cw* = 10 *μm* and 20 *μm* while keeping the depth constant at *Cd* = 1 *mm*

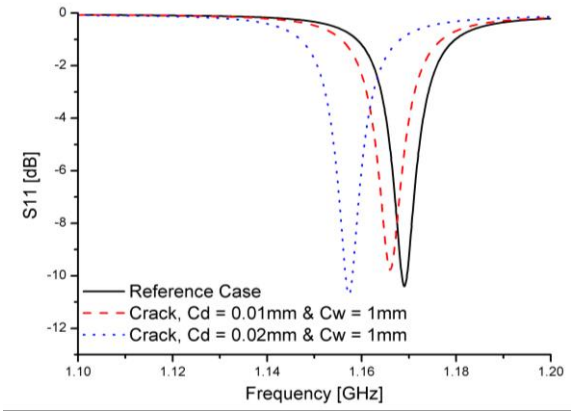

Figure 10. Variation of crack depth *Cd* = 10 *μm* and 20 *μm* while keeping the width at *Cw* = 1 *mm*

4. Conclusion

The procedures of designing enhanced coupling symmetrical split ring resonator (SSRR) with spurlines have been explained in detail in this paper. The designed SSRR sensor is based on Microstrip planar resonator. The electric field distributions and the location of the material under test (MUT) have been also demonstrated. The mechanism of sensing is explained and a minimum of reflected coefficient (*S11*) at resonance frequency shifts whenever the enhanced SSRR is loaded. A maximum shift of more than 96 MHZ is achieved when the crack depth and width kept at 2 *mm*. The minimum detection of limit is investigated which is a round 10 *μm* width or depth where the minimum shift of reflected frequency is recorded at 6.2 MHz and 3 MHz for crack width and depth respectively. The most significant findings from this study is the sensor's capability of sensing sub-millimeter crack on aluminum metallic plate which can be applied in very important industrial applications. Future work can be done by verifying and validating the simulated results through experimental works.

Acknowledgments

This work was supported in part by UTeM Zamalah Scheme and in part by Universiti Teknikal Malaysia Melaka (UTeM).

References

[1] Alahnomi RA, Zakaria Z, Ruslan E, Ab Rashid SR, Mohd Bahar AA, Shaaban A. Microwave bio-sensor based on symmetrical split ring resonator with spurline filters for therapeutic goods detection. PLoS One. 2017;12(9).
[2] Alahnomi RA, Zakaria Z, Yussof ZM, Sutikno T. Determination of solid material permittivity using T-ring resonator for food industry. TELKOMNIKA. 2019;17(1):489–97.
[3] Alahnomi R, Binti N, Hamid A, Zakaria Z, Sutikno T, Azuan A. Microwave Planar Sensor for Permittivity Determination of Dielectric Materials. Indones J Electr Eng Comput Sci. 2018;11(1): 362–71.
[4] Alhegazi A, Zakaria Z, Shairi NA, Sutikno T, Alahnomi RA. Analysis and Investigation of a Novel Microwave Sensor with High Q-Factor for Oil Sensing. Indones J Electr Eng Comput Sci. 2018;12(3):1407–12.
[5] Azuan A, Bahar M, Zakaria Z, Rashid SRA, Isa AAM, Alahnomi RA, et al. Dielectric Analysis of Liquid Solvents Using Microwave Resonator Sensor For High Efficiency Measurement. Microw Opt Technol Lett. 2017;59(2):367–71.
[6] Azuan A, Bahar M, Zakaria Z, Rosmaniza S, Rashid A, Isa AA. Microstrip Planar Resonator Sensors

for Accurate Dielectric Measurement of microfluidic solutions. 3rd Int Conf Electron Des. 2016; 416–21.
[7] Ismail MK, Zakaria Z, Hassan N, Yik SW, Mawardy M. Microwave Planar Sensor for Determination of the Permittivity of Dielectric Material. Bull Electr Eng Informatics. 2018;7(4):640–9.
[8] Wei Z, Huang J, Li J, Xu G, Ju Z, Liu X, et al. A High-Sensitivity Microfluidic Sensor Based on a Substrate Integrated Waveguide Re-Entrant Cavity for Complex Permittivity Measurement of Liquids. Sensors. 2018;18.
[9] Saadat-safa M, Ramahi OM. Full Characterization of Magneto-Dielectric Materials Using a Novel CSRR Based Sensor. 2018 9th Int Symp Telecommun. 2018;442–6.
[10] Zhang X, Ruan C, Haq T ul, Chen K. High-Sensitivity Microwave Sensor for Liquid Characterization Using a Complementary Circular Spiral Resonator. sensors. 2019;19.
[11] Alahnomi RA, Zakaria Z, Ruslan E, Isa AAM, Bahar AAM. Optimization Analysis of Microwave Ring Resonator for Bio-sensing Application. Int J Appl Eng Res. 2015;10(7):18395–406.
[12] Albishi AM, Ramahi OM. Microwaves-Based High Sensitivity Sensors for Crack Detection in Metallic Materials. IEEE Trans Microw Theory Tech. 2017;65(5):1864–72.
[13] Yadav R, Member S, Patel PN. Characterization of High-Frequency Dielectric Laminates Using a Scanning-Probe Based on EBG Structure. IEEE Trans Instrum Meas. 2017;1–9.
[14] Nesić D. Microstrip Resonator with Slotted Ground Plane for Detecting Lateral Position. J Electr Eng. 2016;67(5):383–6.
[15] Kaur A, Marwaha A. Complementary Split Ring Resonator Based Sensor for Crack Detection. Int J Electr Comput Eng. 2015;5(5):1012–7.
[16] Ali A, Hu B, Ramahi O. Intelligent detection of cracks in metallic surfaces using a waveguide sensor loaded with metamaterial elements. Sensors (Switzerland). 2015;15(5):11402–16.
[17] Albishi A, Ramahi OM. Detection of surface and subsurface cracks in metallic and non-metallic materials using a complementary split-ring resonator. Sensors (Switzerland). 2014;14(10):19354–70.
[18] Albishi AM, Boybay MS, Ramahi OM. Complementary split-ring resonator for crack detection in metallic surfaces. IEEE Microw Wirel Components Lett. 2012;22(6):330–2.
[19] Alahnomi RA, Zakaria Z, Ruslan E, Rashid SRA, Bahar AAM. High-Q Sensor Based on Symmetrical Split Ring Resonator with Spurlines for Solids Material Detection. IEEE Sensors [Internet]. 2017;17(9):2766–75. Available from: http://ieeexplore.ieee.org/abstract/document/7879244/
[20] Alahnomi RA, Zakaria Z, Ruslan E, Rashid SRA, Azuan A, Bahar M. Investigation of Symmetrical Split Ring Resonator (SSRR) Couplings for Material Characterization. IEEE Asia-Pacific Conf Appl Electromagn. 2016;(December):11–3.
[21] Alahnomi RA, Zakaria Z, Ruslan E, Isa AAM. Optimization Analysis of Microwave Ring Resonator for Bio-sensing Application. Int J Appl Eng Res. 2015;10(7):18395–406.
[22] Chang K, Hsieh LH. Microwave Ring Circuits and Related Structures. 2nd Edi. John Wiley & Sons. John Wiley & Sons, Inc; 2004.
[23] Huang Y, Boyle K. Antennas From Theory To Practice. First Edit. John Wiley & Sons Ltd; 2008.
[24] Ansari MAH, Jha AK, Akhtar MJ. Permittivity Measurement of Common Solvents Using the CSRR Based Sensor. Antennas Propag Usn Natl Radio Sci Meet 2015 IEEE Int Symp. 2015;1(2):1199–200.
[25] Jinhu Zhou, Peng Jia, Yanqin Zhang XH. High sensitive biosensor based on aSRR and high-impedance microstrip line. Proc 2013 2nd Int Conf Meas Inf Control [Internet]. 2013 Aug;234–7. Available from: http://ieeexplore.ieee.org/lpdocs/epic03/wrapper.htm?arnumber=6757955
[26] Angkawisittpan N. Miniaturization of bandstop filter using double spurlines and double stubs. Przegląd Elektrotechniczny (Electrical Rev. 2012;(11):178–81.